

## Rapid Communications

*Rapid Communications are intended for the accelerated publication of important new results and are therefore given priority treatment both in the editorial office and in production. A Rapid Communication in Physical Review B should be no longer than four printed pages and must be accompanied by an abstract. Page proofs are sent to authors.*

Electronic structure of  $\text{Si}_{46}$  and  $\text{Na}_2\text{Ba}_6\text{Si}_{46}$ 

Susumu Saito

Department of Physics, Tokyo Institute of Technology, 2-12-1 Oh-okayama, Meguro-ku, Tokyo 152, Japan

Atsushi Oshiyama

Fundamental Research Laboratories, NEC Corporation, 34 Miyukigaoka, Tsukuba, Ibaraki 305, Japan

(Received 16 September 1994)

We study solids of  $\text{Si}_{20}$  fullerenes,  $\text{Si}_{46}$  and  $\text{Na}_2\text{Ba}_6\text{Si}_{46}$ , in the framework of density-functional theory. The electronic structure of  $\text{Si}_{46}$  is remarkably different from that of the diamond Si lattice due to its pentagonal network. The valence-band top becomes deeper, resulting in a narrow valence-band width and a wide fundamental gap. Also, another gap appears within the valence bands. In the Na- and Ba-codoped phase, Ba states show strong hybridization with  $\text{Si}_{46}$  states giving a very high Fermi-level density of states, which should be of essential importance for the superconductivity observed in  $\text{Na}_x\text{Ba}_y\text{Si}_{46}$ .

The dodecahedral-cage cluster of 20 atoms with icosahedral symmetry ( $I_h$ ) was previously proposed for C, Si, and Ge by using the  $sp^3$  model potential<sup>1</sup> and the electronic structure of the  $\text{Si}_{20}$  cluster obtained in the local-density approximation within the density-functional theory (LDA) (Ref. 2) was reported.<sup>3</sup> Later, this dodecahedral cluster was pointed out to be the smallest possible fullerene cage with 12 pentagons and no hexagons.<sup>4</sup> On the other hand, the tetrahedrally coordinated Si (or Ge) materials crystallized with alkali-metal atoms were reported to consist of polyhedral units.<sup>5</sup> These polyhedra are now more familiar to us as fullerene cages. The unit cell of  $\text{Na}_8\text{Si}_{46}$ , for example, consists of six tetrakaidecahedra corresponding to  $\text{C}_{24}$ ,<sup>6</sup> or  $\text{Si}_{24}$ , and two dodecahedra corresponding to the above  $\text{Si}_{20}$ . More recently, the synthesis of  $\text{Na}_x\text{Ba}_y\text{Si}_{46}$  was reported<sup>7</sup> and in this system superconductivity was observed finally in the material with the tetrahedrally bonded Si network.<sup>8</sup>

In the present paper, we report the electronic structure of pristine  $\text{Si}_{46}$ , which is pointed out to be essentially the body-centered-cubic (bcc) lattice of  $\text{Si}_{20}$  fullerenes, and of Na- and Ba-doped  $\text{Si}_{46}$ ,  $\text{Na}_2\text{Ba}_6\text{Si}_{46}$ , obtained within the LDA. Although all Si atoms are tetrahedrally coordinated in  $\text{Si}_{46}$ , its electronic structure is found to be remarkably different from that of the diamond Si lattice ( $\text{Si}_2$ ): The valence band becomes narrow, a new gap appears within the valence bands, and the fundamental gap becomes wider by 0.72 eV compared with the  $\text{Si}_2$  lattice to be in the visible-light energy region. These are the consequences of the pentagonal network of tetrahedrally bonded Si atoms. In the case of  $\text{Na}_2\text{Ba}_6\text{Si}_{46}$ , on the other hand, the charge transfer from alkali-metal atom (Na) to fullerene cages and the hybridization between the alkaline-earth atom (Ba) states and the

$\text{Si}_{46}$  conduction-band states are found to take place, giving the metallic electronic structure as in the case of metal-doped solid  $\text{C}_{60}$ .<sup>9,10</sup> In addition, the Fermi-level density of states is found to become very high due to this hybridization. Hence, doping alkaline-earth metal atoms into  $\text{Si}_{46}$  should be very important for the occurrence of the superconductivity.

In Fig. 1, the geometry of (metal-doped)  $\text{Si}_{46}$  is shown. From the viewpoint of the polyhedral space filling, the tetrakaidecahedron is a major polyhedron. However, they share faces with one another, while dodecahedra do not. Hence, it is more natural to consider not  $\text{Si}_{24}$  but  $\text{Si}_{20}$  to be a constructing unit of the  $\text{Si}_{46}$  lattice as discussed in the following. In  $\text{Si}_{46}$ ,  $\text{Si}_{20}$  fullerenes form the bcc lattice and due to the interfullerene Si—Si bonds eight atoms in each  $\text{Si}_{20}$  are tetrahedrally coordinated. The bcc lattice has six distorted tetrahedral interstitial sites per lattice point and half of them are occupied by additional Si atoms. Then, due to bonds between these interstitial-site atoms and  $\text{Si}_{20}$ ,  $\text{Si}_{20}$  fullerenes show the complete orientational ordering with  $90^\circ$  rotation of the center  $\text{Si}_{20}$  and at the same time the remaining 12 Si atoms of each  $\text{Si}_{20}$  as well as the interstitial-site Si atoms are also tetrahedrally coordinated. The geometry of this  $(\text{Si}_3\text{Si}_{20})_2$ , or  $\text{Si}_{46}$ , is optimized here within the LDA.

In the case of  $\text{Na}_2\text{Ba}_6\text{Si}_{46}$ , Na atoms are trapped inside the  $\text{Si}_{20}$  fullerene and Ba atoms occupy remaining three interstitial sites (per  $\text{Si}_{20}$ ) which are not filled by the interstitial Si atoms. This is an ideal-composition phase derived from the Rietveld refinement data for  $\text{Na}_x\text{Ba}_y\text{Si}_{46}$ , which was recently synthesized and is found to show superconductivity with the transition temperature ( $T_c$ ) of about 4 K.<sup>8</sup> Since the interstitial-site Ba atoms are also surrounded by 24 Si atoms forming the second-smallest fullerene-cage network, the sys-

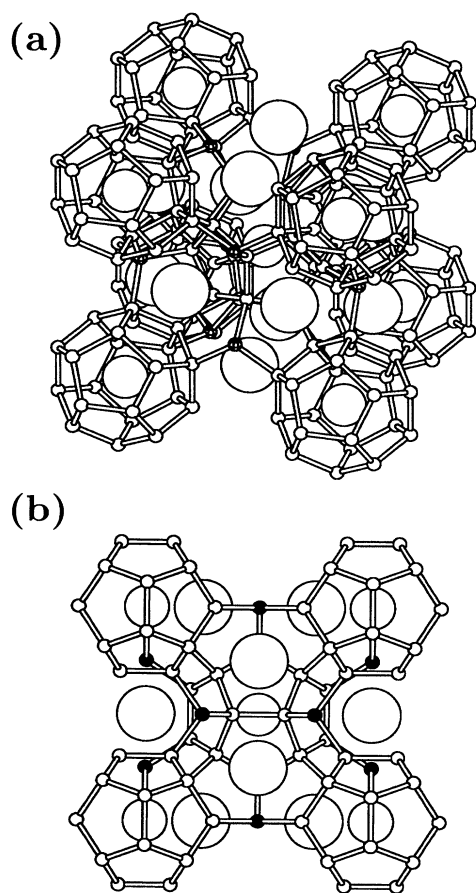


FIG. 1. (a)  $\text{Si}_{46}$  lattice with Na (smaller open spheres) and Ba (larger open spheres) ( $\text{Na}_2\text{Ba}_6\text{Si}_{46}$ ) consisting of the bcc lattice of  $I_h$   $\text{Si}_{20}$  fullerenes and interstitial-site Si atoms (small hatched spheres). Ba and Na atoms occupy the interstitial site and the  $\text{Si}_{20}$  center site, respectively. Eight  $\text{Si}_{20}$  fullerenes on the cube corners and one more  $\text{Si}_{20}$  at the cube center with  $90^\circ$  rotation are drawn. The geometry of the pristine  $\text{Si}_{46}$  has been optimized in the LDA and is found to be stable even without metal atoms (see text). (b) Its top view.

tem is stable in air unlike metal-doped solid  $\text{C}_{60}$  superconductors. It should be noted that this  $\text{Na}_2\text{Ba}_6\text{Si}_{46}$  and A15-phase  $\text{Ba}_3\text{C}_{60}$  (Ref. 11) are isostructural materials belonging to the same simple-cubic space group  $Pm\bar{3}n$ . In  $\text{Na}_2\text{Ba}_6\text{Si}_{46}$ , or  $(\text{Ba}_3\text{Si}_3\text{Na@Si}_{20})_2$  ( $\text{Na@Si}_{20}$  denotes an endohedral metal-fullerene complex), the  $I_h$   $\text{Na@Si}_{20}$  forms the bcc lattice as in the case of the  $I_h$   $\text{C}_{60}$  in  $\text{Ba}_3\text{C}_{60}$ , or  $(\text{Ba}_3\text{C}_{60})_2$ , with equivalent alternative orientational ordering. Moreover, Ba positions are also equivalent in two materials. In addition, in  $(\text{Ba}_3\text{Si}_3\text{Na@Si}_{20})_2$ , vacant interstitial sites of  $(\text{Ba}_3\text{C}_{60})_2$  are occupied by Si atoms. In the electronic-structure calculation, the lattice constant (10.26 Å) as well as the Si atom positions experimentally reported for  $\text{Na}_x\text{Ba}_y\text{Si}_{46}$  (Ref. 7) are used. Its structural parameters are very similar to those optimized for the pristine  $\text{Si}_{46}$ .

As for the exchange-correlation potential in the LDA, Ceperley-Alder potential<sup>12</sup> is used. The conjugate-gradient procedure for the self-consistent electronic-structure calcula-

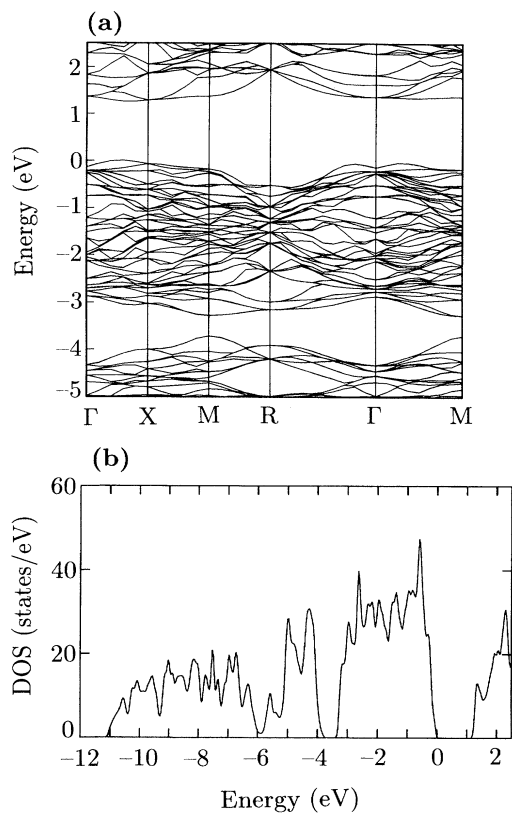


FIG. 2. (a) Band structure and (b) density of states of  $\text{Si}_{46}$ . Energy is measured from the valence-band top.

tion and, in the case of  $\text{Si}_{46}$ , also for the geometry optimization is adopted.<sup>13</sup> Norm-conserving pseudopotentials<sup>14</sup> and plane-wave basis set with the cutoff energy of 8 Ry for geometry optimization and 16 Ry for the electronic-structure and the cohesive-energy calculations are used. For comparison, we have also calculated the electronic structure and the cohesive energy of the diamond  $\text{Si}_2$  lattice.

At the optimized geometry, the lattice constant of  $\text{Si}_{46}$  obtained is 10.19 Å, being identical to the experimental value of  $\text{Na}_8\text{Si}_{46}$  (Ref. 5) and corresponding to the 15% larger volume per atom than that of the  $\text{Si}_2$  lattice. Bond lengths are 2.356 Å (48 bonds per unit cell), 2.392 Å (12 bonds), 2.338 Å (8 bonds), and 2.282 Å (24 bonds). The average value 2.366 Å is slightly (0.6%) longer than the bond length of the  $\text{Si}_2$  lattice. Bond angles distribute in the range from  $105.3^\circ$  to  $124.5^\circ$ . However, due to the softness of the bond-bending distortion modes, the cohesive energy of the  $\text{Si}_{46}$  lattice obtained is as large as 5.86 eV per atom, being less than that of the  $\text{Si}_2$  lattice by only 0.09 eV per atom.

In Fig. 2, the band structure and the density of states of  $\text{Si}_{46}$  obtained are shown. Since all the Si atoms are tetrahedrally coordinated as in the case of the  $\text{Si}_2$  lattice,  $\text{Si}_{46}$  becomes semiconducting. However, surprisingly, the electronic structure of  $\text{Si}_{46}$  is remarkably different from that of the  $\text{Si}_2$  consisting also of tetrahedrally bonded Si atoms. The total width of the valence band (about 11 eV) is considerably narrower than that of the  $\text{Si}_2$  lattice (11.9 eV). Furthermore, a new gap within the valence band opens in addition to the

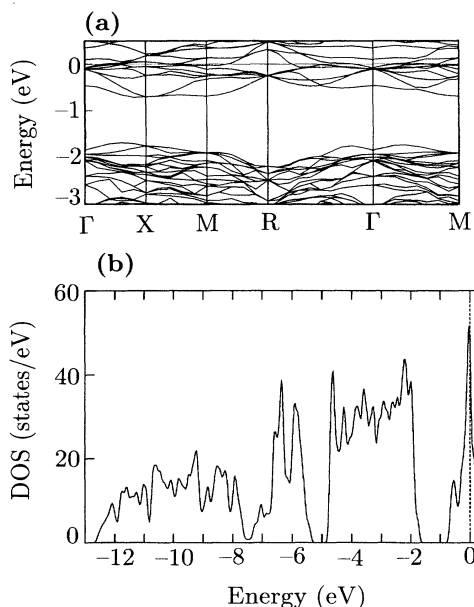


FIG. 3. (a) Band structure around the fundamental gap and (b) density of states of  $\text{Na}_2\text{Ba}_6\text{Si}_{46}$ . Energy is measured from the Fermi level which is denoted by a thin horizontal line in (a) and by a vertical broken line in (b).

fundamental gap between the valence band and the conduction band. The fundamental-gap value obtained 1.26 eV is much larger than that of the  $\text{Si}_2$  lattice (0.54 eV). Although the LDA usually underestimates the gap value, the difference between two cases suggests that  $\text{Si}_{46}$  would have a gap of about 1.9 eV considering the experimental gap of the  $\text{Si}_2$  (1.17 eV).<sup>15</sup> This estimated value is comparable to that of the porous Si and is in a visible-light energy range. Both the valence-band top and the conduction-band bottom are located on the  $\Gamma X$  ( $\Delta$ ) line, and are very close in  $\mathbf{k}$  space, although the direct transition between the highest valence band and the lowest conduction band is optically forbidden. Orientationally averaged effective masses at these points are  $m_h=0.61$  and  $m_e=0.73$  in units of the bare electron mass.<sup>16</sup>

Above-mentioned remarkable differences in the electronic structure of  $\text{Si}_{46}$  and  $\text{Si}_2$  can be attributed to the difference in their ring statistics: in the  $\text{Si}_{46}$  lattice 87% are fivefold rings and only 13% are sixfold rings in sharp contrast to the  $\text{Si}_2$  diamond lattice in which all the rings are sixfold. On the tetrahedrally coordinated Si lattice, the lower and upper halves of the valence band are expected to consist mainly of the Si 3s and 3p states, respectively.<sup>17</sup> On the sixfold-ring diamond lattice, the s orbitals can form a complete antibonding state having a node on all the bonds. Therefore, in the  $\text{Si}_2$  lattice, 3s-like states can distribute up to high energy and are merged with the lower 3p-like states giving the continuous valence band.<sup>17</sup> On the fivefold-ring lattice, on the other hand, s orbitals cannot form a complete antibonding state unlike the diamond lattice. In the case of the  $\text{Si}_{46}$  lattice, therefore, the highest 3s-like state is considerably lower in energy than that of the  $\text{Si}_2$  lattice and becomes lower than the lowest 3p-like state, and a new gap between the s-like states and the p-like states opens. Similar consideration for the

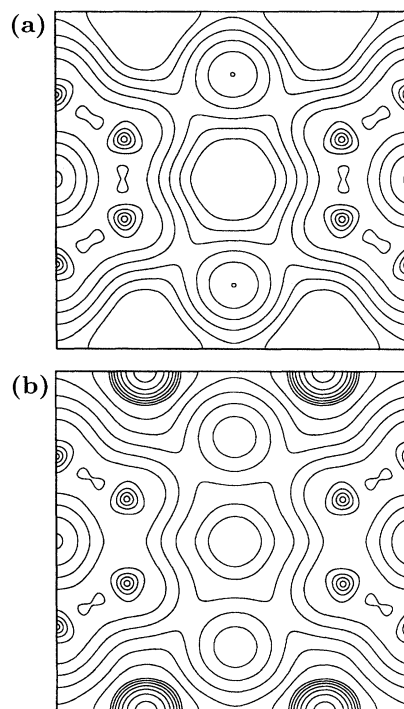


FIG. 4. Contour maps of the valence-electron densities of (a)  $\text{Si}_{46}$  and (b)  $\text{Na}_2\text{Ba}_6\text{Si}_{46}$  on the (100) plane. Each contour represents twice (half) the density of the neighboring contours. In (a), eight steepest-gradient narrow areas correspond to the core regions of Si atoms forming half hexagons on both sides of the figure. The center of the figure corresponds to the center of the empty  $\text{Si}_{20}$  cage, above and below which there are relatively high-density spherical regions corresponding to the charge forming Si—Si bonds perpendicular to this plane. In (b), the Na atom is at the center of the  $\text{Si}_{20}$  cage, i.e., the center of the figure, which still belongs to the lowest-density region. Along the top line of the figure, there are two Ba atom sites surrounded by the high charge density region. There are two Ba atoms also along the bottom line.

bonding orbitals suggests that the valence-band top of  $\text{Si}_{46}$  is lower than that of the diamond  $\text{Si}_2$  lattice, which explains the narrow whole valence-band width as well as the wider fundamental gap.

This fundamental gap becomes narrow due to the enhancement of the screening effect in  $\text{Na}_2\text{Ba}_6\text{Si}_{46}$  where 14 (total number of valence electrons of Na and Ba atoms) electrons occupy the conduction band (Fig. 3). Although the valence-band density of states of  $\text{Na}_2\text{Ba}_6\text{Si}_{46}$  is more or less similar to that of the pristine  $\text{Si}_{46}$ , the conduction-band density of states shows strong modification upon the inclusion of metal atoms and the Fermi-level density of states,  $N(E_F)$ , becomes very high, 47.9 (states/eV) with 0.1 eV Gaussian broadening, which is about twice higher than the value expected from the simple filling of the conduction band of  $\text{Si}_{46}$  [Fig. 2(b)] by 14 electrons. This is a consequence of the strong hybridization between the  $\text{Si}_{46}$  conduction-band states and the Ba and/or Na states.

In Fig. 4, the valence-electron densities of  $\text{Si}_{46}$  and  $\text{Na}_2\text{Ba}_6\text{Si}_{46}$  are shown. It is evident that there remains considerable charge around the Ba site in contrast to the lowest

electron density around the Na site. Therefore, the Ba state is expected to be hybridized much more strongly with the  $\text{Si}_{46}$  conduction-band state than the Na state. In the case of superconducting doped solid  $\text{C}_{60}$ , a similar behavior, i.e., a nearly complete charge transfer from alkali atoms to the fullerene cage and a strong hybridization between the alkaline-earth atom states and the fullerene states, are found to take place.<sup>9,10</sup> Since the Ba  $5d$  state rather than the  $6s$  state is believed to be more strongly hybridized with the fullerene state, the Ba  $5d$  state would also play a very important role in the hybridization with the  $\text{Si}_{46}$  states to give the high  $N(E_F)$  in  $\text{Na}_2\text{Ba}_6\text{Si}_{46}$ . As in the case of  $A_3\text{C}_{60}$  ( $A = \text{K}, \text{Rb}$ , etc.),<sup>9</sup> the high  $N(E_F)$  found in Ba-doped  $\text{Si}_{46}$  should be very important for the occurrence of the superconductivity observed in  $\text{Na}_x\text{Ba}_y\text{Si}_{46}$ . This also explains the absence of the superconducting behavior in  $\text{Na}_8\text{Si}_{46}$  down to 2 K.<sup>18</sup>

Although the high-pressure metallic phases of Si, i.e.,  $\beta$ -Sn and simple-hexagonal phases, are known to show superconductivity with  $T_c$  of around 6–8 K,<sup>19</sup>  $\text{Na}_x\text{Ba}_y\text{Si}_{46}$  is the first example of the superconducting tetrahedrally coordinated Si network. It can be also regarded as a superconducting heavily doped semiconductor discussed years ago.<sup>20</sup> Hence, the doped solid  $\text{Si}_{20}$  may belong to a new class of superconducting materials to be studied in the future. Since the Ba state is hybridized with the  $\text{Si}_{46}$  conduction-band states, the Sr-doped  $\text{Si}_{46}$  will show a different superconducting transition temperature because of the different hybridization strength expected. The replacement of Ba by Sr or other alkaline-earth atoms may have an influence on the superconducting behavior also through the lattice vibration. Phonon modes involving alkaline-earth atoms would couple with the conduction electrons due to the hybridization discussed above.

A very small total-energy difference in  $\text{Si}_{46}$  and  $\text{Si}_2$  ob-

tained indicates that the production of the semiconducting  $\text{Si}_{46}$  would be possible and it should be highly stable once it were formed. To synthesize  $\text{Ar}_x\text{Si}_{46}$  and  $\text{Xe}_x\text{Si}_{46}$  might be also possible. They should be electronically very similar to the pristine  $\text{Si}_{46}$ . Also  $\text{Ge}_{46}$  would be an interesting material to be studied. Since alkali-doped  $\text{Ge}_{46}$  has been already produced,<sup>5</sup> the synthesis of  $\text{Na}_x\text{Ba}_y\text{Ge}_{46}$  would be possible. In the case of carbon, on the other hand, the metal-doped  $\text{C}_{46}$  has not been synthesized yet. However, once it were formed,  $\text{C}_{46}$  would be stable as in the case of diamond, the known stable tetrahedrally coordinated solid carbon being slightly higher in total energy than the ground-state structure, i.e., graphite. The metal-doped  $\text{C}_{46}$ ,  $\text{Na}_2\text{Ca}_6\text{C}_{46}$ , for example, would be metallic and is a good candidate for the higher- $T_c$  superconductor due to the high phonon frequency and the strong electron-phonon interaction generally expected for carbon materials. In addition, some metal-doped  $\text{C}_{46}$  lattices may be harder than the pristine  $\text{C}_{46}$  which would be already as hard as diamond.<sup>21</sup> Such “metallic diamonds” should be useful in extreme conditions and are of significant importance in the wide field of material science and engineering.

Pristine and doped solid  $\text{C}_{60}$  are found to be not only geometrically but also electronically hierarchical materials<sup>9,10,22</sup> having many interesting properties. Now  $\text{Si}_{46}$  consisting mainly of  $\text{Si}_{20}$  fullerenes is found to show superconductivity upon metal doping. This again demonstrates the rich physical properties of the hierarchical fullerene-based materials. Dodecahedral fullerenes,  $\text{C}_{20}$ ,  $\text{Si}_{20}$ , and  $\text{Ge}_{20}$ , will open a new field in fullerene science in the near future.

We would like to thank Professor S. Yamanaka for communicating his results prior to publication.

- <sup>1</sup>S. Saito, S. Ohnishi, and S. Sugano, *Phys. Rev. B* **33**, 7036 (1986).
- <sup>2</sup>P. Hohenberg and W. Kohn, *Phys. Rev.* **136**, B864 (1964); W. Kohn and L. J. Sham, *ibid.* **140**, A1133 (1965).
- <sup>3</sup>S. Saito and S. Ohnishi, in *Microclusters*, edited by Y. Nishina, S. Ohnishi, and S. Sugano (Springer-Verlag, Berlin, 1987), p. 263.
- <sup>4</sup>D. J. Klein, W. A. Seitz, and T. G. Schmalz, *Nature (London)* **323**, 703 (1986).
- <sup>5</sup>C. Cros, M. Pouchard, and E. P. Hagenmuller, *J. Solid State Chem.* **2**, 570 (1970).
- <sup>6</sup>H. W. Kroto, *Nature (London)* **329**, 529 (1987).
- <sup>7</sup>S. Yamanaka, H. Horie, H. Nakano, and M. Ishikawa, *Fullerene Sci. Technol.* (to be published).
- <sup>8</sup>H. Kawaji, H. Horie, S. Yamanaka, and M. Ishikawa, *Phys. Rev. Lett.* (to be published).
- <sup>9</sup>S. Saito and A. Oshiyama, *Phys. Rev. B* **44**, 11 536 (1991); *J. Phys. Chem. Solids* **54**, 1759 (1993).
- <sup>10</sup>S. Saito and A. Oshiyama, *Phys. Rev. Lett.* **71**, 121 (1993).
- <sup>11</sup>A. R. Kortan, N. Kopylov, R. M. Fleming, O. Zhou, F. A. Thiel, and R. C. Haddon, *Phys. Rev. B* **47**, 13 070 (1993).
- <sup>12</sup>J. P. Perdew and A. Zunger, *Phys. Rev. B* **23**, 5048 (1981).
- <sup>13</sup>O. Sugino and A. Oshiyama, *Phys. Rev. Lett.* **68**, 1858 (1993).
- <sup>14</sup>N. Troullier and J. L. Martins, *Phys. Rev. B* **43**, 1993 (1991); L.

- Kleinman and D. M. Bylander, *Phys. Rev. Lett.* **48**, 1425 (1982).
- <sup>15</sup>*Zahlenwerte und Funktionen aus Naturwissenschaften und Technik*, edited by O. Madelung, M. Schulz, and H. Weiss, Landolt-Börnstein, New Series, Group III, Vol. 17, Pt. a (Springer-Verlag, New York, 1982).
- <sup>16</sup>Recently, the electronic structure of  $\text{Si}_{46}$  has been studied using the *ab initio* tight-binding-like molecular dynamics method and a slightly different band structure has been reported [G. B. Adams, M. O’Keeffe, A. A. Demkov, O. F. Sankey, and Y.-M. Huang, *Phys. Rev. B* **49**, 8048 (1994)].
- <sup>17</sup>D. A. Papaconstantopoulos, *Handbook of the Band Structure of Elemental Solids* (Plenum, New York, 1986).
- <sup>18</sup>S. B. Roy, K. E. Sim, and A. D. Caplin, *Philos. Mag. B* **65**, 1445 (1992).
- <sup>19</sup>K. J. Chang, M. M. Dacorogna, M. L. Cohen, J. M. Mignot, G. Chouteau, and G. Martinez, *Phys. Rev. Lett.* **54**, 2375 (1985).
- <sup>20</sup>M. L. Cohen, in *Superconductivity*, edited by R. D. Parks (Marcel Dekker, New York, 1969), p. 615.
- <sup>21</sup>The pristine  $\text{Si}_{46}$  is found to be as hard as the  $\text{Si}_2$  lattice, although the accurate evaluation of its bulk modulus requires higher cut-off energy.
- <sup>22</sup>S. Saito and A. Oshiyama, *Phys. Rev. Lett.* **66**, 2637 (1991).